



Published in final edited form as:

Stem Cells. 2015 June ; 33(6): 1719–1729. doi:10.1002/stem.1974.

Integrin $\alpha 6\beta 1$ Expressed in ESCs Instructs the Differentiation to Endothelial Cells

Sophie P. Toya^{1,2,3}, Kishore K. Wary^{1,3}, Manish Mittal^{1,3}, Fei Li^{1,3}, Peter T. Toth¹, Changwon Park^{1,3}, Jalees Rehman^{1,2,3}, and Asrar B. Malik^{1,3}

¹Department of Pharmacology, University of Illinois College of Medicine, Chicago

²Department of Medicine, University of Illinois College of Medicine, Chicago

³Center for Lung and Vascular Biology, University of Illinois College of Medicine, Chicago

Abstract

Adhesion of embryonic stem cells (ESCs) to the extracellular matrix (ECM) may influence differentiation potential and cell fate decisions. Here we investigated the inductive role of binding of integrin $\alpha 6\beta 1$ expressed in mouse (m)ESCs to laminin-1 (LN1) in mediating the differentiation of ESCs to endothelial cells (ECs). We observed that $\alpha 6\beta 1$ binding to LN1 was required for differentiation to ECs. $\alpha 6\beta 1$ functioned by recruiting the adaptor tetraspanin protein CD151, which activated FAK and Akt signaling and mediated the EC lineage-specifying transcription factor Er71. In contrast, association of the ESC-expressed $\alpha 3\beta 1$, another highly expressed LN1 binding integrin, with CD151, prevented $\alpha 6\beta 1$ -mediated differentiation. CD151 thus functioned as a bifurcation router to direct ESCs towards ECs when $\alpha 6\beta 1$ associated with CD151, or prevented transition to ECs when $\alpha 3\beta 1$ associated with CD151. These observations were recapitulated in mice in which *$\alpha 6$* integrin or *CD151* knockdown reduced the expression of Er71-regulated angiogenesis genes and development of blood vessels. Thus, interaction of $\alpha 6\beta 1$ in ESCs with LN1 activates $\alpha 6\beta 1$ /CD151 signaling which programs ESCs towards the EC lineage fate.

Keywords

integrins; laminin-1; stem cells; tetraspanins; stem cell endothelial differentiation; gene regulation

INTRODUCTION

Interactions of extracellular matrix (ECM) proteins with integrins and downstream activation of signaling pathways regulate cellular processes as diverse as cell motility, cell-cell and cell-matrix adhesion, and cell polarity [1,2]. It is known that binding of fibroblasts

Corresponding Authors Asrar B. Malik, abmalik@uic.edu; Kishore K. Wary, kkwary@uic.edu.

Author contributions

ST, ABM, JR and KW designed the experiments; ST and MM performed the experiments. ST, ABM, JR and KW analyzed the data and wrote the manuscript. FL assisted in ESC differentiation experiments. PT assisted with the microscopy experiments, and CP advised on the Er71 component of the studies.

Conflict of Interest

The authors have no conflicts of financial interest to declare.

and other cell types to ECM activates “outside-in” signals depending on the specific matrix protein on which cells are adherent [3–5]. However, the role of integrin-ECM interactions in programming of embryonic stem cells (ESCs) to specific cell fates is not well understood [6,7]. While ESCs have the potential to differentiate into endothelial cells (ECs) [8–11], the contribution of specific ECM proteins and the signaling mechanisms responsible for EC differentiation and lineage specification remain incompletely understood [12–17].

Studies have shown that ECs emerge from ESCs upon applying mesodermal differentiating conditions [18–20]. The generated ECs are characterized by upregulation of *Fetal liver kinase-1 (Flk1) gene* and EC-specific adherens junction *VE-cadherin gene* [21–25]. Differentiation towards the EC fate also requires activation of specific transcriptional factors such as Er71/Etv2, which binds Flk1 and VE-cadherin promoters [21–25]. In addition, growth factors such as BMP-4 (bone morphogenetic protein 4) and VEGF are also important cues for the transition towards ECs [21,22].

Here we investigated the role of the ESC-expressed integrins $\alpha 3\beta 1$ and $\alpha 6\beta 1$ in mediating the differentiation to ECs. Studies focused on the question whether ESCs grown on laminin-1 (LN1) could be coaxed into transitioning into ECs, and if so, the signaling mechanisms responsible, and whether the generated ECs were capable of forming blood vessels. Laminins are a prominent ESC niche [26,27] in developmental vasculogenesis [28]. Since differentiation of ECs may recapitulate the vascular differentiation program [20,25], we surmised that ESC-expressed $\alpha 3\beta 1$ and $\alpha 6\beta 1$ interacting with LN1 are important in generating ECs capable of forming functional blood vessels. LN1 binding integrins, in addition to binding ECM proteins, also associate with the adaptor protein CD151, known as the 4-pass transmembrane protein tetraspanin-4 (TMSF4), which regulates signaling downstream of integrin activation [29–35]. As CD151 interacting with $\alpha 3\beta 1$ or $\alpha 6\beta 1$ [30–35] is capable of directing signaling towards distinct pathways [30–34], we also investigated the role of CD151 through binding with either $\alpha 3\beta 1$ or $\alpha 6\beta 1$ in the mechanism of transition of ESCs to ECs.

MATERIALS AND METHODS

Immunofluorescence Staining and Microscopy

These assays were performed as described [20,36]. Briefly, mESCs were fixed with 4% PFA, permeabilized, and stained with rat anti-mouse $\alpha 6$, rabbit anti-mouse CD151, or goat anti-mouse $\alpha 3$ antibodies. Frozen sections were stained with rat anti-mouse Er71. Paraffin sections were stained for Hematoxylin/Eosin (H/E). Fluorescent images were acquired at room temperature with a Zeiss LSM 710 META confocal laser scanning microscope using an α -Plan-Apochromat 63x/1.46NA, (1.5x zoom factor) or a C-Apochromat 63x/1.2NA objective, (2.6x Zoom factor). The Zeiss Zen software was used for image acquisition. Co-localization was analyzed using ImageJ (NIH) with the Fiji plug-in *coloc_2* [37]. Background subtraction was performed to eliminate nonspecific staining. The calculation of the fractions of CD151 that overlapped with integrins was performed using thresholded Mander’s coefficient. H/E images were taken by an Olympus BX51 microscope with an Olympus 12.5MP DP71 CCD camera using a UPlanFL N dry 40X/0.75NA objective. Super Resolution imaging was performed at Northwestern University Cell

Imaging Facility using Delta Vision-OMX Super Resolution Fluorescent Microscope (supported by NIH Grant S10OD010777, Thomas J. Hope).

Cell Surface Integrin Internalization Assays

Internalization of $\alpha 6$ integrin was determined by cell surface biotinylation assay. Cell surface biotinylation experiments have been previously described [35,36]. In brief, cells were plated (5×10^5) on 35mm dishes coated with 0.2 μ g/ml LN-1. The cells were washed with cold PBS and incubated with reducible sulfo-NHS-SS-biotin (Pierce, Rockford, IL). To strip the biotin bound to surface proteins, the cells were treated for 30min on ice with a reducing solution containing 42mM glutathione (reduced form), 75mM NaCl, 75mM NaOH, and 1% BSA (called quencher). Some dishes were left untreated to measure the total amount of labeled integrin. For $\alpha 6$ integrin co-IP, the cells were solubilized in 1% Brij-99 and 150mM NaCl lysis buffer at 4°C. Cell surface biotinylated integrins were analyzed by streptavidin-HRP, subjected to chemiluminescence (ECL), and signals were quantitated by densitometric analysis. Alternatively, to determine cell surface $\alpha 6$ integrin, mESCs were washed with cold PBS and then incubated with various concentrations of trypsin (1–100U/ml in PBS) at RT. To stop digestion, 1mM phenylmethylsulfonyl fluoride (PMSF) was added, cells washed and lysed in Brij-99+150mM NaCl lysis buffer. For immunoblotting, anti- $\alpha 6$ antibody recognizing an extracellular domain of $\alpha 6$ ($\alpha 6$ -ecto) or anti- $\alpha 6$ antibody recognizing the cytoplasmic C-terminal ($\alpha 6$ -cyto, clone H-87, Santa Cruz Biotechnology, sc-10730) region of the integrin were used.

Transfection Experiments

Transfection with $\alpha 6$ siRNA, *CD151* siRNA and $\alpha 3$ siRNA was performed in 24-well plates using pooled specific mouse integrin $\alpha 6$ siRNA (Dharmacon, Thermo Scientific, Accell SmartPool mouse Itga6, E-040204-00-0005, Accell SmartPool mouse *cd151*, E-043064-00-0005, Accell SmartPool mouse Itga3, E-042246-00-0005) and a non-targeting control siRNA (Dharmacon, Thermo Scientific, Accell non-targeting Control Pool, D-001910-10-05) (25nM final concentration). The mESCs were transfected in triplicate for 24hr in the presence of serum free media, and then 500 μ l of complete growth media was added per well for another 24 hr. Then, the transfection mix was replaced with fresh growth media, and protein expression analysis was performed. Transfection with dominant-negative-Akt (HA-Akt DN, [K179M], Addgene plasmid 16243) and with Gst-Er71 (vector pGEX-4T1, provided by Dr. C. Park) was performed using Lipofectin Transfection Reagent (Life Technologies™).

RESULTS

LN1 interaction with mESC-expressing $\alpha 6\beta 1$ induces differentiation towards EC fate

Integrin subunits $\alpha 6$ and $\beta 1$ were predominantly expressed transcripts in mESCs (Figure S1A). Flow cytometry analysis verified high cell surface expression of $\alpha 6$ and $\beta 1$ (Figure 1A). In contrast, $\beta 4$, another $\alpha 6$ binding partner, was not seen (Figure 1B). mESC adhesion to LN1, but not to control gelatin matrix, was significantly reduced using anti- $\alpha 6$ blocking antibody (clone GoH3) (Figure 1C). We determined whether binding of $\alpha 6\beta 1$ to LN1 regulated the differentiation of mESCs to ECs as compared to differentiation on type IV

collagen. mESC were plated at low density on either type IV collagen or LN1 in presence of defined EC differentiation medium containing VEGF165 [20]. Cells seeded at similar densities (3×10^3 cells/cm²) under both conditions expressed Flk1 and VE-cadherin on day#3 with levels peaking on day#6–7. Importantly, differentiation on LN1 was significantly more efficient with 25% of cells on LN-1 becoming Flk1⁺VE-cadherin⁺ compared to only 8% double positive cells on type IV collagen (Figure 1D).

We next examined the consequences of inhibiting $\alpha 6$ expression on mESC differentiation (Figure S1B). $\alpha 6$ knockdown was associated with significantly impaired proliferation (Figure 1E) and increased apoptosis (Figure 1F) consistent with a prominent role of $\alpha 6$ in ESC maintenance [17]. To avoid confounding effects of apoptosis in these experiments, we used a blocking antibody against $\alpha 6$ (clone GoH3). In pilot experiments we employed a range of doses of the $\alpha 6$ blocking antibody determining, for each particular dose, the activation status of $\alpha 6\beta 1$ as reflected by the decrease in the mean fluorescence intensity of the activation dependent antibody against $\beta 1$, clone 9EG7 [39] (i.e. % $\beta 1$ inhibition, Figure S1C). At an antibody dosage inducing $\alpha 6\beta 1$ inhibition of 40%, mESCs did not undergo apoptosis (Figure S1D); importantly, these cells failed to differentiate into ECs on LN1 substrate as determined by suppressed mRNA and protein expression of FIK1 three days after onset of differentiation (Figure 1G) and significantly reduced number of Flk1⁺VE-cadherin⁺ ECs at day#6 (Figure 1H). Thus, $\alpha 6\beta 1$ interaction with LN-1 appears to be a crucial mechanism of differentiating mESCs into ECs.

mESCs differentiation into ECs requires interaction of $\alpha 6\beta 1$ with CD151

To address signaling mechanisms downstream of $\alpha 6\beta 1$ mediating ESC differentiation to ECs, we examined the role of the tetraspanin CD151, key regulator of $\alpha 6\beta 1$ signaling [32,33,35]. CD151 interacted with $\alpha 6\beta 1$ on plating mESCs on LN1 but not following mESC plating on type IV collagen (Figure 2A). mESCs were transfected with *CD151*-siRNA to address the role of CD151 in $\alpha 6\beta 1$ -activated signaling (Figure S2A). Control experiments showed that *CD151*-knockdown alone had no effect on expression of $\alpha 6$ (Figure S2B) and cell viability (Figure S2C) whereas CD151 depletion significantly reduced the emergence of ECs with only 6% of cells becoming Flk1⁺VE-cadherin⁺ by day#6 as compared to 25% double positive cells in control experiments (Figure 2B, left and middle panels, and Figure 1D).

In other studies, mESCs were transfected with siRNA targeting *CD151*, and tyrosine phosphorylation of the $\alpha 6$ effectors, FAK and Akt [40–42], was determined. Deletion of *CD151* reduced tyrosine phosphorylation of both FAK and Akt in contrast to controls (Figures 2C, 2D). Further, transfection of the constitutively-active FAK mutant (CD2-FAK) [43] in *CD151*-depleted mESCs restored FAK activation (Figure S2D) as well as differentiation of mESCs into ECs (Figure 2B, right panel); thus, CD151 activation downstream of $\alpha 6\beta 1$ functioned through FAK and Akt signaling to induce mESC differentiation to ECs.

To further address the role of CD151 in mediating the emergence of ECs, we undertook biotinylation studies of cell surface $\alpha 6\beta 1$ on day#3 of differentiation. mESCs were labeled with reducible biotin on ice and returned to 37°C; at 5, 10, and 20 min the cells were treated

with impermeable glutathione to strip biotin from the cell surface followed by cell lysis and analysis by IP of internalized $\alpha 6\beta 1$ retaining the biotin label. We observed that $\alpha 6\beta 1$ was internalized in ESCs differentiating to ECs and the response was significantly reduced in the absence of CD151 (Figure 2E), suggesting the crucial role of CD151-mediated $\alpha 6\beta 1$ internalization in signaling mESC differentiation into ECs.

$\alpha 3\beta 1$ interaction with CD151 prevents mESCs differentiation into ECs

Besides $\alpha 6$, $\alpha 3$ and $\alpha 7$ are the two other LN1-binding integrins forming heterodimers with $\beta 1$ [44]. As $\alpha 7$ was not detected during the 6-day differentiation period (Figure S3A), we addressed whether $\alpha 3\beta 1$ also has a role in signaling the emergence of ECs. $\alpha 3$ expression increased on day#3 after the onset of differentiation (Figure S3A). Interestingly, treating ESCs with anti- $\alpha 3$ integrin blocking antibody [45,46] beginning on day#3 and continuing until day#6 significantly enhanced the differentiation of mESCs to ECs (Figure 3A). A similar enhanced EC differentiation was recapitulated on transfecting ESCs with $\alpha 3$ siRNA (Figure S3B and S3C). Co-IP studies using mESCs lysates obtained on day#3 showed that $\alpha 3$ interacted with CD151 (Figure 3B). Interestingly, binding of $\alpha 3$ to CD151 was stronger than binding of $\alpha 6$ to CD151 as evident by the requirement for stringent cell lysis condition using 1% NP-40 to disrupt $\alpha 3$ /CD151 interaction as opposed to $\alpha 6$ /CD151 interaction.

Since CD151 competes with binding to both $\alpha 6$ $\alpha 3$ integrins [47,48], we next addressed the possibility that CD151 binding to $\alpha 3$ influenced CD151 binding to $\alpha 6$. Day#3 cells exposed to increasing concentrations of anti- $\alpha 3$ integrin blocking antibody overnight were lysed and subjected to IP for CD151 and $\alpha 6$. We observed increased association between the two proteins at the highest concentrations of $\alpha 3$ blocking antibody or in the presence of $\alpha 3$ knockdown (Figure 3C), consistent with a competition between the two integrins for binding to CD151. This observation was confirmed by immunostaining using day #3 mESCs differentiating on LN1 exposed to anti- $\alpha 3$ integrin blocking antibody and stained for CD151 and either $\alpha 3$ or $\alpha 6$. The prominent co-localization of $\alpha 3$ with CD151 seen at baseline, was reduced on exposing to $\alpha 3$ blocking antibody; in contrast, co-localization of $\alpha 6$ with CD151 increased on exposing to the anti- $\alpha 3$ antibody (Figure 3D) further consistent with competition of $\alpha 3$ and $\alpha 6$ for binding to CD151.

To address whether $\alpha 3$ regulates the internalization of $\alpha 6$ described above, we determined the consequences of $\alpha 3$ blockade on cell surface expression of $\alpha 6$. On day#3 of differentiation, cells were treated with increasing concentrations of anti- $\alpha 3$ integrin blocking antibody, and subsequently with 50U trypsin to detach any cell surface-associated $\alpha 6$. Immunoblotting using an antibody recognizing only the extracellular $\alpha 6$ domain showed that $\alpha 3$ blockade decreased the susceptibility of cell surface $\alpha 6$ to trypsin cleavage (Figure 3E, upper panel). At the same time, the intracellular C-terminal domain of $\alpha 6$ was unaffected in both $\alpha 3$ -blocked and control cells (Figure 3E, lower panel). Thus, $\alpha 3$ functioned by preventing internalization of $\alpha 6$ and, thereby, inhibiting $\alpha 6$ mediated differentiation of mESCs to ECs.

Because CD151 contains the YRSL motif recognized by Adaptor Protein-2 (AP-2) in the C-terminal domain, the core component of the clathrin endocytic machinery [33], we investigated whether association of $\alpha 3\beta 1$ or $\alpha 6\beta 1$ with CD151 regulated internalization of

integrins via clathrin-mediated endocytosis. Co-IP of $\alpha 3$ and $\alpha 6$ with heavy chain (HC) clathrin showed association between $\alpha 3$ and clathrin HC in control cells, which decreased with increasing concentrations of anti- $\alpha 3$ blocking antibody and was coincident with onset of $\alpha 6$ association with CD151 (Figures 3F, 3G). Depletion of CD151 prevented clathrin binding for both $\alpha 3$ and $\alpha 6$ (Figures 3F, 3G) consistent with a role of CD151 as a bifurcation point for $\alpha 3$ and $\alpha 6$ signaling. Immunostaining studies showed that co-localization of $\alpha 6$ with clathrin was enhanced by increasing the availability of CD151 after blocking $\alpha 3$, and inhibited by CD151-depletion (Figure 3H), confirming the biochemical results. These findings show that $\alpha 3$ and $\alpha 6$ competed for association with CD151 and association of $\alpha 6$ with a core clathrin component regulated endocytosis of $\alpha 6$ following the interaction of $\alpha 6$ with CD151.

$\alpha 6\beta 1$ signaling activates Er71 leading to EC lineage specification

To determine the function of internalized $\alpha 6$ in mediating FAK activation and thereby signaling the differentiation of ESCs to ECs, we assessed tyrosine phosphorylation of FAK. For these experiments, we sorted day#3 cells for Flk1 expression and exposed Flk1⁺ cells for various times to $\alpha 3$ integrin blocking antibody. Both FAK and Akt phosphorylation were increased (Figure 4A, 4B). In addition, we observed that activation of Akt inhibited activation of Erk1/2 in the same time frame (Figure 4C). These results demonstrate that $\alpha 6$ internalization plays a crucial role in signaling ESC differentiation to ECs whereas $\alpha 3$ represses $\alpha 6$ signaling to prevent differentiation of ECs.

Next, we addressed whether differentiation towards ECs required activation of the transcription factor Er71, known to induce differentiation of stem cells into Flk1⁺ ECs through binding to *Flk1* and *VE-cadherin* promoters [21–25]. We determined whether $\alpha 3$ blockade and resultant $\alpha 6$ signaling activated Er71. These studies demonstrated Er71 activation was indeed a function of $\alpha 6$ signaling (Figure 4D, 4E) consistent with the role of $\alpha 6$ in the induction of ECs.

As activation of Akt downstream of $\alpha 6$ may be important in signaling EC differentiation [49], we addressed the role of Akt in the activation of transcriptionally-competent Er71. In mESCs transfected with dominant negative Akt (DN-Akt) (Figures S4A, S4B) or with GST-*Er71* plasmid (Figure S4C) to upregulate Er71 expression, we observed significantly reduced Er71 phosphorylation in the presence of dominant negative Akt in contrast to controls (Figure 5A). Further, we observed direct association of Akt with Er71 (Figure 5B) supporting a role of Akt in contributing to Er71 activation during ESCs differentiation. mESCs transfection with dominant negative Akt resulted in defective ESCs differentiation into ECs (Figure 5C, left panel) which could not be rescued by co-transfection with GST-*Er71* plasmid (Figure 5C, middle panel) whereas transfection with *Er71* in the presence of active Akt induced marked differentiation (Figure 5B, right panel) indicating upstream activity of Akt on Er71. Transfection with *Er71*-empty vector had no effect on differentiation in control experiments (Figure S4D). These observations were further supported by determination of nuclear localization of Er71 in DN-Akt-transfected cells, which was reduced as compared to control cells (Figure 5D), indicating that active Akt was required for Er71 transcriptional activity.

$\alpha 6\beta 1$ /CD151 pathway activates Er71 signaling and vasculogenesis *in vivo*

We next evaluated whether disruption of $\alpha 6$ integrin function modified Er71 upregulation *in vivo*. We transfected mESCs with siRNA directed against integrin $\alpha 6$ or *CD151* and transplanted them subcutaneously in immunocompromised mice. Cell masses were excised on day#3 and day#10. On day#3 after transplantation, using whole tissue RT-PCR (Figure 6A) and immunohistochemistry (Figure 6B), we observed down regulation of *Er71* and decreased Er71 protein expression in cells in which either $\alpha 6$ or *CD151* were depleted, in association with impaired Er71 nuclear localization. These results suggested impaired activation of Er71 transcriptional activity in the absence of $\alpha 6$ or CD151. On day#10, teratomas formed from mESCs bearing $\alpha 6$ or *CD151* siRNA and control mESCs were excised and histologically examined. All formed tumors contained all three embryonic layers (Figure S4A). Teratomas from $\alpha 6$ -and *CD151*-depleted cells were smaller (Figure 6C) and contained fewer vessels than controls (Figure 6D). To quantify effects of disruption of $\alpha 6$ /*CD151*, we performed RT PCR for the common mesodermal marker *Brachyury* as well as for genes known to be regulated by Er71, i.e., *Vegfa*, *Tie2* and *VE-cadherin (Cdh5)* [24]. Although expression of *Brachyury* was not significantly different compared to scrambled controls (Figure 6E), we observed significant differences in expression of Er71 regulated genes with downregulation in $\alpha 6$ -and CD151-depleted cells (Figure 6F). To determine whether overexpression of Er71 rescued defect in angiogenesis, we co-transfected mESCs with siRNA against *CD151* and with GST-*Er71* (Figure S4B). Both tumor size and vascularity were restored by overexpression of Er71 (Figures 6C, D), whereas expression levels of Er71-controlled genes was restored to control levels (Figure 6F) supporting the role of Er71 and upstream $\alpha 6\beta 1$ /CD151 pathway in mediating vascularization.

DISCUSSION

We demonstrated in the present studies the central role of mESCs expressing integrins $\alpha 3\beta 1$ and $\alpha 6\beta 1$, the binding partners of the ECM protein LN1, in differentially regulating the transition of mESCs to the EC lineage. We identified a $\alpha 3\beta 1$ -dependent “braking” mechanism suppressing EC differentiation whereas $\alpha 6\beta 1$ promoted EC differentiation through activation of the transcription factor Er71. The identified opposing functions of these integrins in differentially regulating mESCs differentiation to ECs were controlled by CD151, which functioned by competitively associating with either $\alpha 3\beta 1$ or $\alpha 6\beta 1$. Signaling activated downstream of $\alpha 6$ interaction with CD151 induced internalization of $\alpha 6$ *via* clathrin-mediated endocytosis, suggesting that $\alpha 6$ internalization is a crucial requirement for signaling the emergence of ECs. $\alpha 6\beta 1$ internalization elicited FAK and Akt signaling, with the latter mediating phosphorylation of Er71. We also demonstrated that mESCs lacking $\alpha 6$ or CD151 were defective in teratoma formation related to impaired vasculogenesis. Moreover, this defect was rescued by over-expression of Er71 suggesting that Er71 is both required and sufficient for $\alpha 6$ /CD151 interaction mediated transition of mESCs to ECs and resultant vasculogenesis. These results together demonstrate the essential role of interaction of ESC-expressed $\alpha 6\beta 1$ with LN1 in generating ECs capable of forming new vessels.

LN1 is known to bind to $\alpha 6\beta 1$ [1,38,44], but the present studies are the first to document the significance of this interaction in ESC differentiation to the EC lineage. $\alpha 6\beta 1$ functioned

secondary to activation of Akt, a pro-survival signal [50]. In addition to the role of Akt in activating EC differentiation through phosphorylation of Er71, it is possible that Akt also plays a role in contributing to the survival of emerging ECs. Thus, we cannot exclude the possibility that both Akt regulated mechanisms are responsible for the observed ESC transition to ECs.

The tetraspanin CD151 was required for $\alpha 6\beta 1$ signaling mediating ESC differentiation into ECs. This was evident from findings that LN1-dependent FAK and Akt signaling were inhibited by CD151 depletion and both FAK activation and EC differentiation were restored by expressing constitutively-active *FAK* mutant in CD151-depleted cells.

We demonstrated that, at the mesodermal progenitor phase, the ESC-expressed $\alpha 3\beta 1$ interacted with CD151 to prevent differentiation towards EC lineage. In contrast, CD151 binding to $\alpha 6$ induced $\alpha 6$ internalization that was dependent on activation of the clathrin endocytic machinery. This finding is consistent with the role of internalization of integrins from the plasma membrane in several integrin regulated processes such as cell adhesion, differentiation, spreading, migration, and invasion [51]. Although $\alpha 3$ and $\alpha 6$ can both associate with a core clathrin component, only $\alpha 6$ was internalized, suggesting that activation of endocytosis of $\alpha 6$ required its interaction with CD151, and hence the $\alpha 6$ signaling responsible for EC differentiation.

We observed that integrin $\alpha 6\beta 1$ competed with $\alpha 3\beta 1$ for binding to CD151. The inhibition of $\alpha 3$ association with CD151 favored the interaction of CD151 with $\alpha 6$, and induced $\alpha 6\beta 1$ -mediated FAK signaling and Er71 phosphorylation. This competitive relationship between $\alpha 3\beta 1$ and $\alpha 6\beta 1$ suggests that CD151 acts as an integrin “toggle switch” regulating the transition to ECs. Indeed, double knockout ($\alpha 3^{-/-}::\alpha 6^{-/-}$) mice have developmental defects not seen in single mutants [52], consistent with opposing signaling functions of $\alpha 3\beta 1$ and $\alpha 6\beta 1$. Studies in which GFP-tagged peptides corresponding to cytoplasmic domain of $\alpha 3$ were injected into LN1-adherent fibroblasts expressing $\alpha 6\beta 1$ integrin showed disengagement of $\alpha 6\beta 1$ integrin [53] consistent with our observations. CD151 was also shown to function as a co-receptor for $\alpha 6\beta 1$ and $\alpha 3\beta 1$ based on its affinity for LN-associated integrins [30–34]. Deletion of CD151 in ECs was accompanied by changes in molecular organization of LN-binding integrins and marked integrin-dependent defects in cell spreading, motility, and 3-dimensional morphology [54,55], pointing to the key role of CD151 interaction with $\alpha 3\beta 1$ or $\alpha 6\beta 1$ in differentially regulating ESCs differentiation to ECs.

Er71 binds to promoters of both VE-cadherin and Flk-1 contributing to the differentiation towards EC lineage [21]. Er71 also acts in concert with the hematopoietic transcription factor Gata2 to promote hematopoietic lineage differentiation at the embryoid body stage [25,56]. Although we did not assess $\alpha 6\beta 1$ -mediated hematopoietic progenitor cell generation, it is possible that LN1 interaction with $\alpha 6\beta 1$ is also involved in hematopoiesis in addition to EC lineage specification as demonstrated.

In summary, our results showed opposing effects of $\alpha 6\beta 1$ and $\alpha 3\beta 1$ through their differential binding to CD151 in regulating the differentiation of ESCs to ECs. Applying the EC

differentiating condition in ESCs induced CD151 binding to $\alpha 6$ resulting in the internalization of $\alpha 6$ and differentiation towards ECs. The complex organized by $\alpha 6\beta 1$ /CD151 interaction was the essential cue for activation of FAK and Akt resulting in phosphorylation of Er71. Thus, our results support a model in which the formation of $\alpha 6\beta 1$ /CD151 complex and activation of FAK and Akt mediate the transition of ESCs to ECs that may have the potential for efficient production of ECs useful for vascular regeneration.

Supplementary Material

Refer to Web version on PubMed Central for supplementary material.

Acknowledgement

Supported by grants from NIH grants HL090152 & HL118068 to ABM, HL119291 to CP, GM094220 to JR, and HL079356 to KKW. ST is recipient of the Parker B. Francis Fellowship

REFERENCES

1. Hynes RO. Integrins: bidirectional, allosteric signaling machines. *Cell*. 2002; 110:673–687. [PubMed: 12297042]
2. Stupack DG, Cheresh DA. ECM remodeling regulates angiogenesis: endothelial integrins look for new ligands. *Sci STKE*. 2002; 119:pe7. [PubMed: 11842241]
3. Lange A, Wickström SA, Jakobson, et al. Integrin-linked kinase is an adaptor with essential functions during mouse development. *Nature*. 2009; 461:1002–1006. [PubMed: 19829382]
4. Mammoto A, Connor KM, Mammoto T, et al. A mechanosensitive transcriptional mechanism that controls angiogenesis. *Nature*. 2009; 457:1103–1108. [PubMed: 19242469]
5. Malanchi I, Santamaria-Martínez A, Susanto E, et al. Interactions between cancer stem cells and their niche govern metastatic colonization. *Nature*. 2011; 481:85–89. [PubMed: 22158103]
6. Streuli CH. Integrins and cell-fate determination. *J Cell Sci*. 2009; 122:171–177. [PubMed: 19118209]
7. Discher DE, Mooney DJ, Zandstra PW. Growth factors, matrices, and forces combine and control stem cells. *Science*. 2009; 324:1673–1677. [PubMed: 19556500]
8. Choi KD, Yu J, Smuga-Otto K, et al. Hematopoietic and endothelial differentiation of human induced pluripotent stem cells. *Stem Cells*. 2009; 27:559–567. [PubMed: 19259936]
9. Yang HM, Moon SH, Choi YS, et al. Therapeutic efficacy of human embryonic stem cell-derived endothelial cells in humanized mouse models harboring a human immune system. *Arterioscler Thromb Vasc Biol*. 2013; 33:2839–2849. [PubMed: 24092748]
10. Adams WJ, Zhang Y, Cloutier J, et al. Functional vascular endothelium derived from human induced pluripotent stem cells. *Stem Cell Reports*. 2013; 1:105–113. [PubMed: 24052946]
11. Prasain N, Lee MR, Vemula S, et al. Differentiation of human pluripotent stem cells to cells similar to cord-blood endothelial colony-forming cells. *Nat Biotechnol*. 2014; 32:1151–1157. [PubMed: 25306246]
12. Tanentzapf G, Devenport D, Godt D, Brown NH. Integrin-dependent anchoring of a stem-cell niche. *Nat Cell Biol*. 2007; 9:1413–1418. [PubMed: 17982446]
13. Pacilli A, Pasquinelli G. Vascular wall resident progenitor cells: a review. *Exp Cell Res*. 2009; 315:901–914. [PubMed: 19167379]
14. Cheng P, Andersen P, Hassel D, et al. Fibronectin mediates mesendodermal cell fate decisions. *Development*. 2013; 140:2587–2596. [PubMed: 23715551]
15. Singh MD, Kreiner M, McKimmie CS, et al. Dimeric integrin $\alpha 5\beta 1$ ligands confer morphological and differentiation responses to murine embryonic stem cells. *Biochem Biophys Res Commun*. 2009; 390:716–721. [PubMed: 19833095]

16. Ghosh M, Helm KM, Smith RW, et al. A single cell functions as a tissue-specific stem cell and the in vitro niche-forming cell. *Am J Respir Cell Mol Biol.* 2011; 45:459–469. [PubMed: 21131442]
17. Lathia JD, Gallagher J, Heddleston JM, et al. Integrin alpha 6 regulates glioblastoma stem cells. *Cell Stem Cell.* 2010; 6:421–432. [PubMed: 20452317]
18. James D, Nam HS, Seandel M, et al. Expansion and maintenance of human embryonic stem cell-derived endothelial cells by TGFbeta inhibition is Id1 dependent. *Nat Biotechnol.* 2010; 28:161–166. [PubMed: 20081865]
19. Orlova VV, van den Hil FE, Petrus-Reurer S, et al. Generation, expansion and functional analysis of endothelial cells and pericytes derived from human pluripotent stem cells. *Nat Protoc.* 2014; 9:1514–1531. [PubMed: 24874816]
20. Kohler EE, Wary KK, Li F, et al. Flk1+ and VE-cadherin+ endothelial cells derived from iPSCs recapitulate vascular development during differentiation and display similar angiogenic potential as ESC-derived cells. *PLoS One.* 2013:e85549. [PubMed: 24386480]
21. Lee D, Park C, Lee H, et al. Er71 acts downstream of BMP, Notch, and Wnt signaling in blood and vessel progenitor specification. *Cell Stem Cell.* 2008; 2:497–507. [PubMed: 18462699]
22. Palencia-Desai S, Kohli V, Kang J, et al. Vascular endothelial and endocardial progenitors differentiate as cardiomyocytes in the absence of Etsrp/Etv2 function. *Development.* 2011; 138:4721–4732. [PubMed: 21989916]
23. Kataoka H, Hayashi M, Nakagawa R, et al. Etv2/Er71 induces vascular mesoderm from Flk1+PDGFRα+ primitive mesoderm. *Blood.* 2011; 118:6975–6986. [PubMed: 21911838]
24. Liu F, Kang I, Park C, et al. ER71 specifies Flk-1+ hemangiogenic mesoderm by inhibiting cardiac mesoderm and Wnt signaling. *Blood.* 2012; 119:3295–3305. [PubMed: 22343916]
25. Park C, Kim TM, Malik AB. Transcriptional regulation of endothelial cell and vascular development. *Circ Res.* 2013; 112:1380–1400. [PubMed: 23661712]
26. Domogatskaya A, Rodin S, Boutaud A, et al. Laminin-511 but not -332, -111, or -411 enables mouse embryonic stem cell self-renewal in vitro. *Stem Cells.* 2008; 26:2800–2809. [PubMed: 18757303]
27. Klaffky EJ, Gonzáles IM, Sutherland AE. Trophoblast cells exhibit differential responses to laminin isoforms. *Dev Biol.* 2006; 292:277–289. [PubMed: 16680816]
28. Risau W, Lemmon V. Changes in the vascular extracellular matrix during embryonic vasculogenesis and angiogenesis. *Dev Biol.* 1988; 125:441–450. [PubMed: 3338622]
29. Hemler ME. Tetraspanin functions and associated microdomains. *Nat Rev Mol Cell Biol.* 2005; 6:801–811. [PubMed: 16314869]
30. Yauch RL, Berditchevski F, Harler MB, et al. Highly stoichiometric, stable, and specific association of integrin alpha3beta1 with CD151 provides a major link to phosphatidylinositol-4 kinase, and may regulate cell migration. *Mol Biol Cell.* 1998; 9:2751–2765. [PubMed: 9763442]
31. Stipp CS, Hemler ME. Transmembrane-4-superfamily proteins CD151 and CD81 associate with alpha 3 beta 1 integrin, and selectively contribute to alpha 3 beta 1-dependent neurite outgrowth. *J Cell Sci.* 2000; 113:187–182.
32. Lammerding J, Kazarov AR, Huang H, et al. Tetraspanin CD151 regulates alpha6beta1 integrin adhesion strengthening. *Proc Natl Acad Sci U S A.* 2003; 100:7616–7621. [PubMed: 12805567]
33. Liu L, He B, Liu WM, et al. Tetraspanin CD151 promotes cell migration by regulating integrin trafficking. *J Biol Chem.* 2007; 282:31631–31642. [PubMed: 17716972]
34. Winterwood NE, Varzavand A, Meland MN, et al. A critical role for tetraspanin CD151 in alpha3beta1 and alpha6beta4 integrin-dependent tumor cell functions on laminin-5. *Mol Biol Cell.* 2006; 17:2707–2721. [PubMed: 16571677]
35. Zhang XA, Kazarov AR, Yang X, et al. Function of the tetraspanin CD151-alpha6beta1 integrin complex during cellular morphogenesis. *Mol Biol Cell.* 2002; 13:1–11. [PubMed: 11809818]
36. Kohler EE, Cowan EC, Chatterjee I, et al. NANOG induction of Fetal liver kinase-1 (FLK1) transcription regulates endothelial cell proliferation and angiogenesis. *Blood.* 2011; 117:1761–1769. [PubMed: 21119109]
37. Schindelin J, Arganda-Carreras I, Frise E, et al. Fiji: an open-source platform for biological-image analysis. *Nat Methods.* 2012; 28:676–682. [PubMed: 22743772]

38. Giancotti FG, Ruoslahti E. Integrin signaling. *Science*. 1999; 285:1028–1032. [PubMed: 10446041]
39. Hughes PE, Oertli B, Hansen M, et al. Suppression of integrin activation by activated Ras or Raf does not correlate with bulk activation of ERK MAP kinase. *Mol Biol Cell*. 2002; 13:2256–2265. [PubMed: 12134066]
40. Herzog B, Pellet-Many C, Britton G, et al. VEGF binding to NRP1 is essential for VEGF stimulation of endothelial cell migration, complex formation between NRP1 and VEGFR2, and signaling via FAK Tyr407 phosphorylation. *Mol Biol Cell*. 2011; 22:2766–2776. [PubMed: 21653826]
41. Chen XL, Nam J, Jean C, et al. VEGF-induced vascular permeability is mediated by FAK. *Dev Cell*. 2012; 22:146–157. [PubMed: 22264731]
42. Xia H, Nho RS, Kahm J, et al. Focal adhesion kinase is upstream of phosphatidylinositol 3-kinase/Akt in regulating fibroblast survival in response to contraction of type I collagen matrices via a beta 1 integrin viability signaling pathway. *J Biol Chem*. 2004; 279:33024–33034. [PubMed: 15166238]
43. Oktay M, Wary KK, Dans M, et al. Integrin-mediated activation of focal adhesion kinase is required for signaling to Jun NH2-terminal kinase and progression through the G1 phase of the cell cycle. *J Cell Biol*. 1999; 145:1461–1469. [PubMed: 10385525]
44. Domogatskaya A, Rodin S, Tryggvason K. Functional diversity of laminins. *Annu Rev Cell Dev Biol*. 2012; 28:523–553. [PubMed: 23057746]
45. Chen Y, Lasaitiene D, Gabrielsson BG, et al. Neonatal losartan treatment suppresses renal expression of molecules involved in cell-cell and cell-matrix interactions. *J Am Soc Nephrol*. 2004; 15:1232–1243. [PubMed: 15100363]
46. DeFreitas MF, Yoshida CK, Frazier WA, et al. Identification of integrin $\alpha 3\beta 1$ as a neuronal thrombospondin receptor mediating neurite outgrowth. *Neuron*. 1995; 15:333–343. [PubMed: 7544141]
47. Wright MD, Geary SM, Fitter S, et al. Characterization of mice lacking the tetraspanin superfamily member CD151. *Mol Cell Biol*. 2004; 24:5978–5988. [PubMed: 15199151]
48. Sterk LM, Geuijen CA, van den Berg JG, et al. Association of the tetraspanin CD151 with the laminin-binding integrins $\alpha 3\beta 1$, $\alpha 6\beta 1$, $\alpha 6\beta 4$ and $\alpha 7\beta 1$ in cells in culture and in vivo. *J Cell Sci*. 2002; 115:1161–1173. [PubMed: 11884516]
49. Yu KR, Yang SR, Jung JW, et al. CD49f enhances multipotency and maintains stemness through the direct regulation of OCT4 and SOX2. *Stem Cells*. 2012; 30:876–887. [PubMed: 22311737]
50. Frisch SM, Ruoslahti E. Integrins and anoikis. *Curr Opin Cell Biol*. 1997; 9:701–706. [PubMed: 9330874]
51. Margadant C, Monsur HN, Norman JC, et al. Mechanisms of integrin activation and trafficking. *Curr Opin Cell Biol*. 2011; 23:607–614. [PubMed: 21924601]
52. De Arcangelis A, Mark M, Kreidberg MJ, et al. Synergistic activities of $\alpha 3$ and $\alpha 6$ integrins are required during apical ectodermal ridge formation and organogenesis in the mouse. *Development*. 1999; 126:3957–3968. [PubMed: 10433923]
53. Laplantine E, Vallar L, Mann K, et al. Interaction between the cytodomains of the $\alpha 3$ and $\beta 1$ integrin subunits regulates remodeling of adhesion complexes on laminin. *J Cell Sci*. 2000; 113:1167–1176. [PubMed: 10704368]
54. Takeda Y, Kazarov AR, Butterfield CE, et al. Deletion of tetraspanin CD151 results in decreased pathologic angiogenesis in vivo and in vitro. *Blood*. 2007; 109:1524–1532. [PubMed: 17023588]
55. Takeda Y, Li Q, Kazarov AR, et al. Diminished metastasis in tetraspanin CD151-knockout mice. *Blood*. 2011; 118:464–472. [PubMed: 21536858]
56. Lammerts van Bueren K, Black BL. Regulation of endothelial and hematopoietic development by the ETS transcription factor Etv2. *Curr Opin Hematol*. 2012; 19:199–205. [PubMed: 22406820]

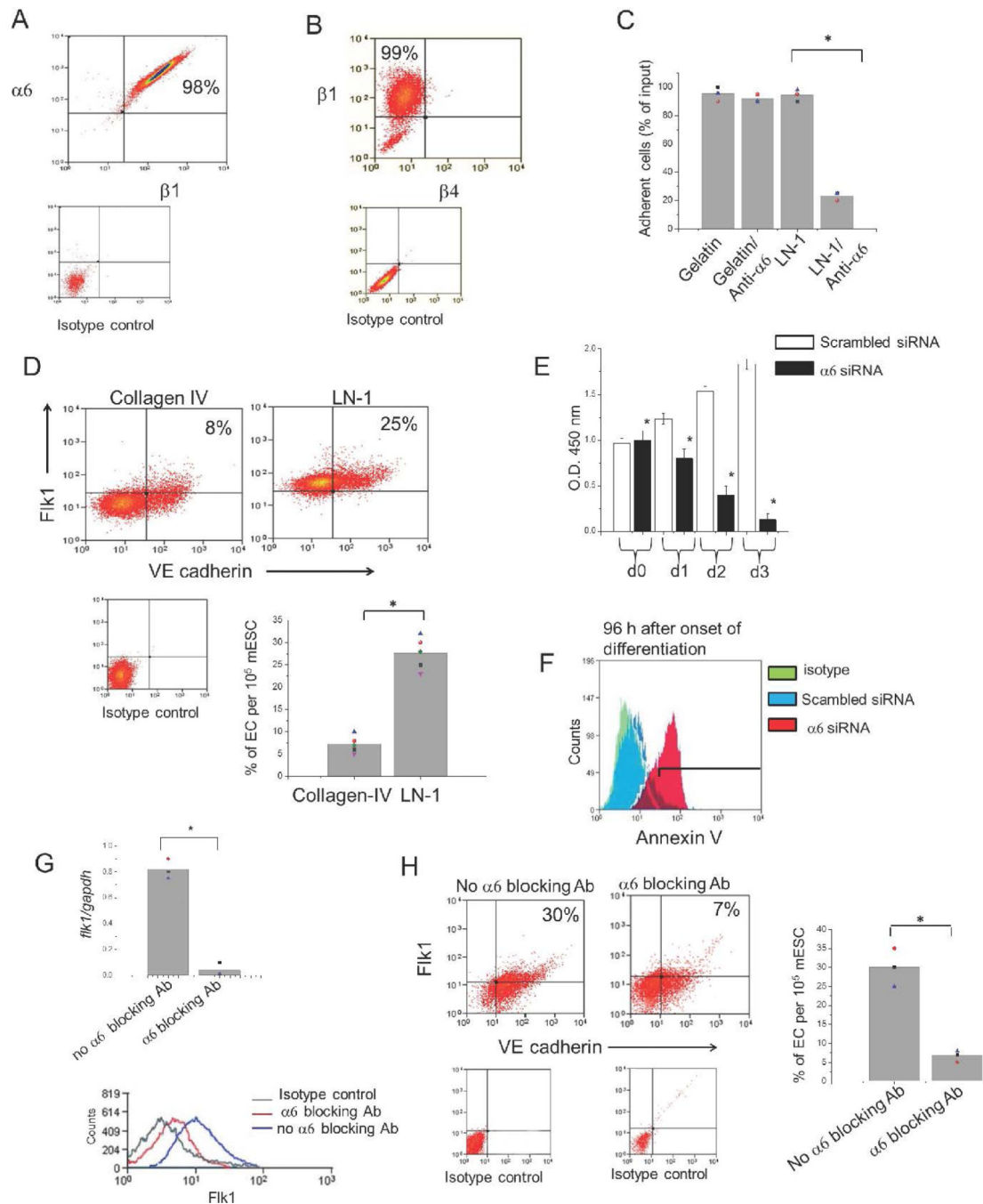


Figure 1. Integrin $\alpha 6$ interaction with LN-1 is required for differentiation of mESCs into Flk1⁺VE-cadherin⁺ECs

(A) Cell surface expression of $\alpha 6$ and $\beta 1$ integrin subunits in mESCs cultured on gelatin.

Plot is representative of 3 separate experiments.

(B) Cell surface expression of $\beta 1$ and $\beta 4$ integrin subunits as determined by flow cytometry of mESCs cultured on gelatin. Plot is representative of 3 separate experiments.

(C) Culture of mESCs in the presence of integrin $\alpha 6$ blocking antibody GoH3 (50 μ g/ml) did not affect adhesion to gelatin, whereas the antibody significantly reduced adhesion to LN-1.

Error bars, mean \pm S.E.M.; * $P < 0.05$, $n = 3$.

(D) mESCs were induced to differentiate in the presence of VEGF165 on Col-IV or LN-1. After 6 days, cell surface expression of EC markers Flk1 and VE-cadherin was determined by flow cytometry. LN-1-differentiated cells were more efficient in giving rise to double positive ECs (25% on LN-1 vs. 8% on Col-IV). Plot is representative of at least 5 separate experiments. Bar graph shows quantitation of Flk1⁺/VE-cadherin⁺ ECs grown on the two substrates. Error bars, mean \pm S.E.M.; * P<0.05.

(E) Transfection of mESC with $\alpha 6$ siRNA led to significant impairment of cell proliferation when compared to scrambled siRNA control as determined by BrdU incorporation. Error bars, mean \pm S.E.M.; * P<0.05, n=3.

(F) Flow cytometric analysis of Annexin V was used as indicator of apoptosis in mESC transfected with $\alpha 6$ siRNA and scrambled control. Knockdown of $\alpha 6$ resulted in enhancement of cell death as determined by Annexin V expression 96 hours after transfection. Plot is representative of 3 separate experiments.

(G) Impaired mesodermal differentiation of mESC treated with anti- $\alpha 6$ blocking antibody, as demonstrated by quantification of *Flk1* transcript and flow cytometry for Flk1 expression three days after onset of mesodermal differentiation compared to non-blocked controls. Error bars, mean \pm S.E.M.; * P<0.05, n=3. Representative plot of Flk1 cell surface expression is shown, (n=3).

(H) Use of anti- $\alpha 6$ blocking antibody resulted in reduced cell surface expression of EC markers Flk1 and VE-cadherin after 6 days of differentiation as determined by flow cytometry. Plot is representative of 3 separate experiments (n=3). Bar graph shows quantitation of Flk1⁺/VE-cadherin⁺ ECs differentiated from blocked mESC and non-blocked controls. Error bars, mean \pm S.E.M.; * P<0.05, n=3.

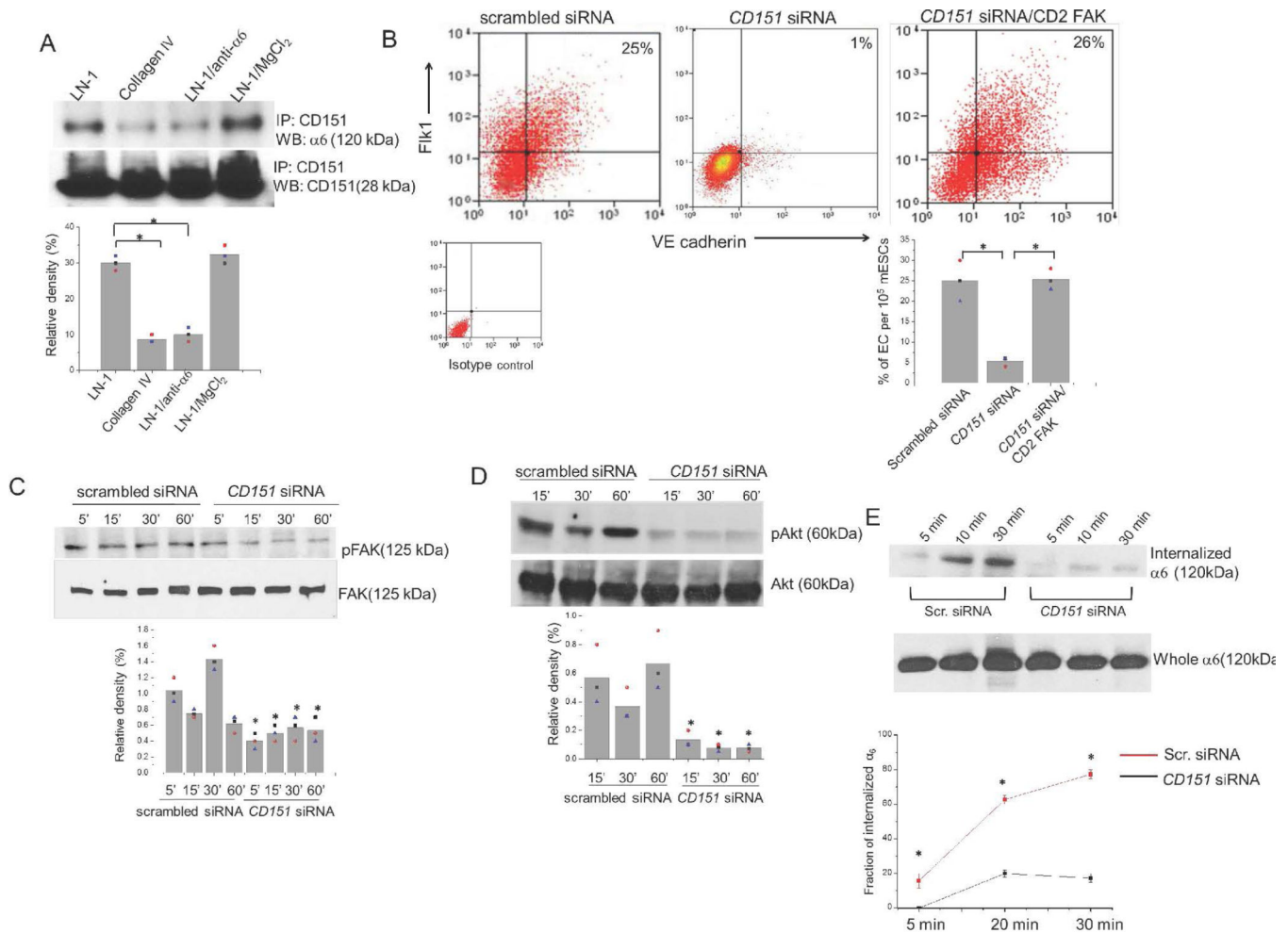


Figure 2. CD151 interaction with $\alpha 6$ activates FAK signaling and mESCs transition into ECs

(A) $\alpha 6$ integrin binds CD151 in LN-1- and activation-dependent manner. Cell extracts prepared from naïve mESCs, plated on either Col-IV or LN-1, were immunoprecipitated with anti-CD151 antibody and immunoblotted for $\alpha 6$. mESCs were cultured under identical conditions in presence of either integrin activator MgCl₂ (0.5 mM) or anti- $\alpha 6$ -blocking antibody (GoH3, 50 μ g/ml). Error bars, mean \pm S.E.M, * P<0.05, n=3.

(B) CD151-knockdown inhibits differentiation of mESCs on LN-1 (middle panel). Restoring FAK activation in CD151-depleted mESCs rescues the defect in emergence of ECs (right panel). Percent (%) of Fik1⁺VE-cadherin⁺ cells on day 6 was the same as in the control group (left panel) and greater than the CD151-depleted group (middle panel). Bar graph shows % Fik1⁺VE-cadherin⁺ cells in the three groups on day 6 of differentiation; Error bars, mean \pm S.E.M, * P<0.05, n=3.

(C, D) CD151-knockdown reduces VEGF-induced phosphorylation of FAK and Akt in mESCs differentiation. Scrambled-siRNA or CD151-knockdown mESCs were exposed to differentiation medium containing VEGF165 for indicated times, and cell extracts were subjected to WB analysis with indicated antibodies.

(E) $\alpha 6$ internalization in differentiating mESC requires CD151. CD151-depleted mESCs and controls underwent biotinylation assay on day#2 of differentiation. At indicated times, cells

were treated with quencher, solubilized, and internalized biotinylated- $\alpha 6$ was subjected to IP with anti- $\alpha 6$ antibody. Non-glutathione-treated day 2 mESCs blotted for $\alpha 6$ were used as controls. Results of 3 individual experiments are plotted as the fraction of internalized $\alpha 6$ over time. Error bars, mean \pm S.E.M.; * $P < 0.05$ vs. controls, $n = 3$.

Author Manuscript

Author Manuscript

Author Manuscript

Author Manuscript

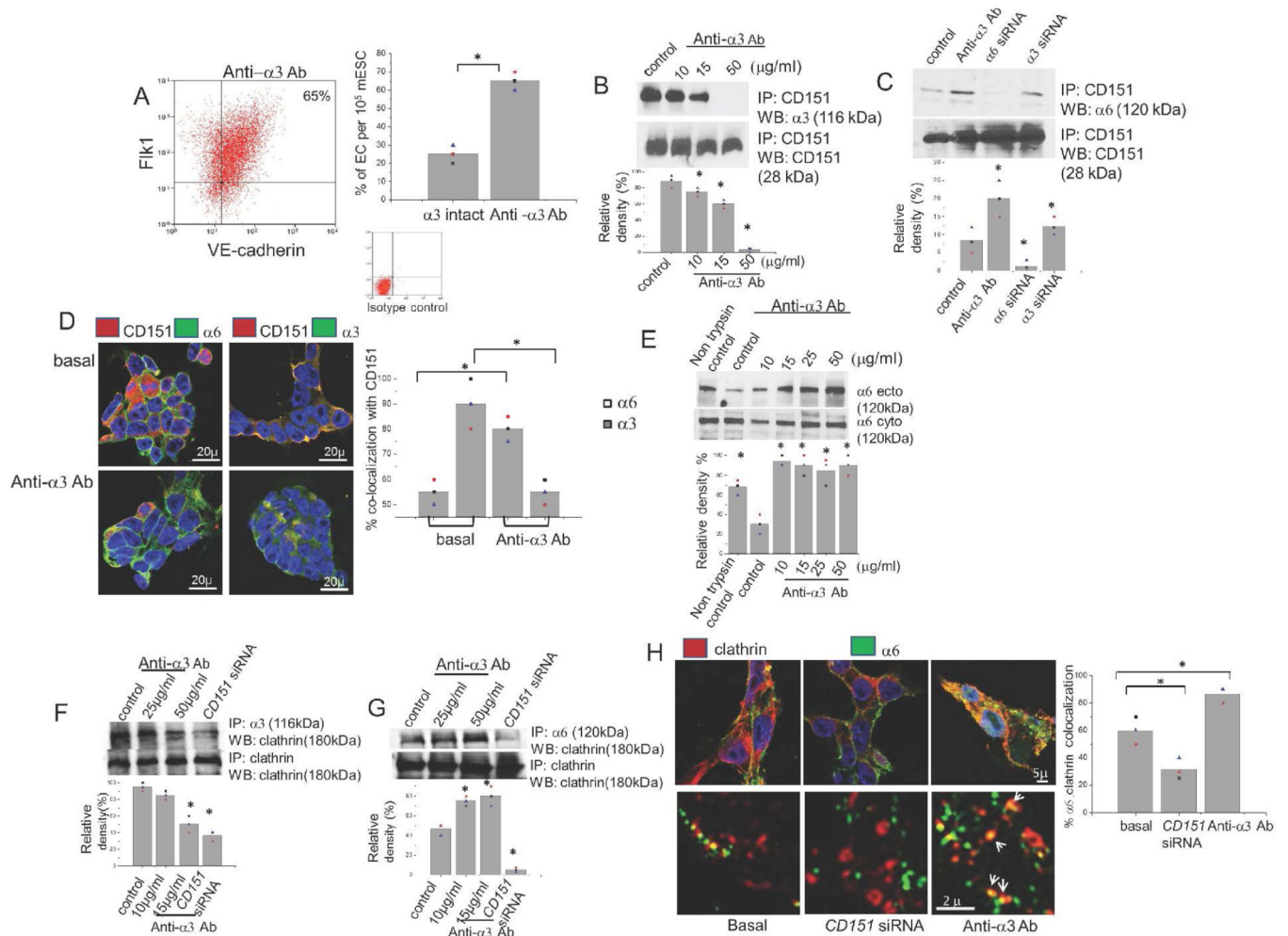


Figure 3. $\alpha 6$ interaction with CD151 is required for differentiation of mESCs to ECs

(A) $\alpha 3$ functions to restrain mESCs differentiation into ECs. Ralph 3.1 ($\alpha 3$ blocking antibody) added daily to differentiating mESCs starting on day#1 increased EC differentiation. Flow cytometry showed an average of 65% Flk1⁺VE-cadherin⁺ cells on day#6. Bar graph represents a comparison of percentages of ECs per 10⁵ mESCs differentiating on LN-1 under control conditions (for comparison see Figure 1D) vs. after addition of Ralph 3.1 to differentiation medium. Error bars, mean \pm S.E.M.; * P<0.05, n=3.

(B) $\alpha 3$ interacts with CD151 in mESCs differentiating into ECs. mESCs at day#3 of differentiation on LN-1 were exposed to 10, 15, or 50 μ g/ml of Ralph 3.1, extracts were immunoprecipitated with anti-CD151 antibody, and analyzed by immunoblotting with anti- $\alpha 3$ antibody. Error bars, mean \pm S.E.M., *P<0.05 comparing 3 different antibody doses vs. control, n=3.

(C) $\alpha 3$ negatively regulates interaction of CD151 with $\alpha 6$. mESCs differentiated for 3 days on LN-1 were either to exposed to $\alpha 3$ blocking antibody overnight or were transfected with $\alpha 3$ siRNA. Cell extracts was immunoprecipitated with anti-CD151 antibody and analyzed by indicated antibody. Error bars, mean \pm S.E.M., * P<0.05, n=3.

(D) Immunostaining of day#3 mESCs plated on LN-1 for CD151, $\alpha 3$, and $\alpha 6$ shows enhanced association of $\alpha 6$ with CD151 upon blockade of $\alpha 3$ For these experiments, day#3

cells were either left untreated or treated with 50 $\mu\text{g}/\text{ml}$ of Ralph 3.1. Graph represents data from 3 independent experiments demonstrating amount of CD151 overlapping with either $\alpha 3$ or $\alpha 6$ integrins basally and after $\alpha 3$ blocking with Ralph 3.1. Results were calculated using thresholded Mander's coefficient. Error bars, mean \pm S.E.M., * $P < 0.05$, $n = 3$. Scale bar, 20 μ . Fluorescent images were acquired with a Zeiss LSM 710 META confocal laser scanning microscope using an α -Plan-Apochromat 63x/1.46NA, (1.5x zoom factor).

(E) $\alpha 3$ negatively regulates $\alpha 6$ internalization. Day#3 mESCs differentiating on LN-1 were treated with increasing doses of Ralph 3.1 and then exposed to 50U of trypsin for 10min at RT. Extracts were analyzed by two different antibodies as indicated. Error bars, mean \pm S.E.M.; $n = 3$, * $P < 0.05$, $n = 3$.

(F) $\alpha 3$ association with clathrin HC is dependent on CD151. CD151-depleted mESCs differentiated for 3 days on LN-1 and control cells were either left untreated or exposed to 25 or 50 $\mu\text{g}/\text{ml}$ with Ralph 3.1 overnight, solubilized, immunoprecipitated for $\alpha 3$, and analyzed by indicated antibody. Error bars, mean \pm S.E.M., $n = 3$, * $P < 0.05$.

(G) $\alpha 6$ association with clathrin heavy chain (HC) is negatively regulated by $\alpha 3$ and enhanced by CD151. In a similar manner as described above cells were immunoprecipitated with anti- $\alpha 6$ and analyzed by indicated antibodies. Error bars, mean \pm S.E.M., * $P < 0.05$, $n = 3$.

(H) CD151 promotes $\alpha 6$ association with clathrin and $\alpha 3$ reduces $\alpha 6$ association with clathrin. Control or CD151-depleted cells were treated with 50 $\mu\text{g}/\text{ml}$ Ralph 3.1, fixed, permeabilized and stained with indicated antibodies. Bar graph represents cumulative data from 3 individual experiments demonstrating $\alpha 6$ overlapping with clathrin basally and on $\alpha 3$ blocking or *CD151* silencing. Results were calculated using Mander's coefficient. Error bars, mean \pm S.E.M., * $P < 0.05$, $n = 3$. Scale bar, 5 μ . Fluorescent images were acquired with a Zeiss LSM 710 META confocal laser scanning microscope using an α -Plan-Apochromat 63x/1.2NA, ((2.6x zoom factor). The lower micrographs represent Super Resolution images acquired using an OMX Structured Illumination Super-Resolution System (Delta Vision) with Plan-Apochromat 63x/1.40 oil DIC objective, a 2.5x zoom factor and 3 SIM rotations.

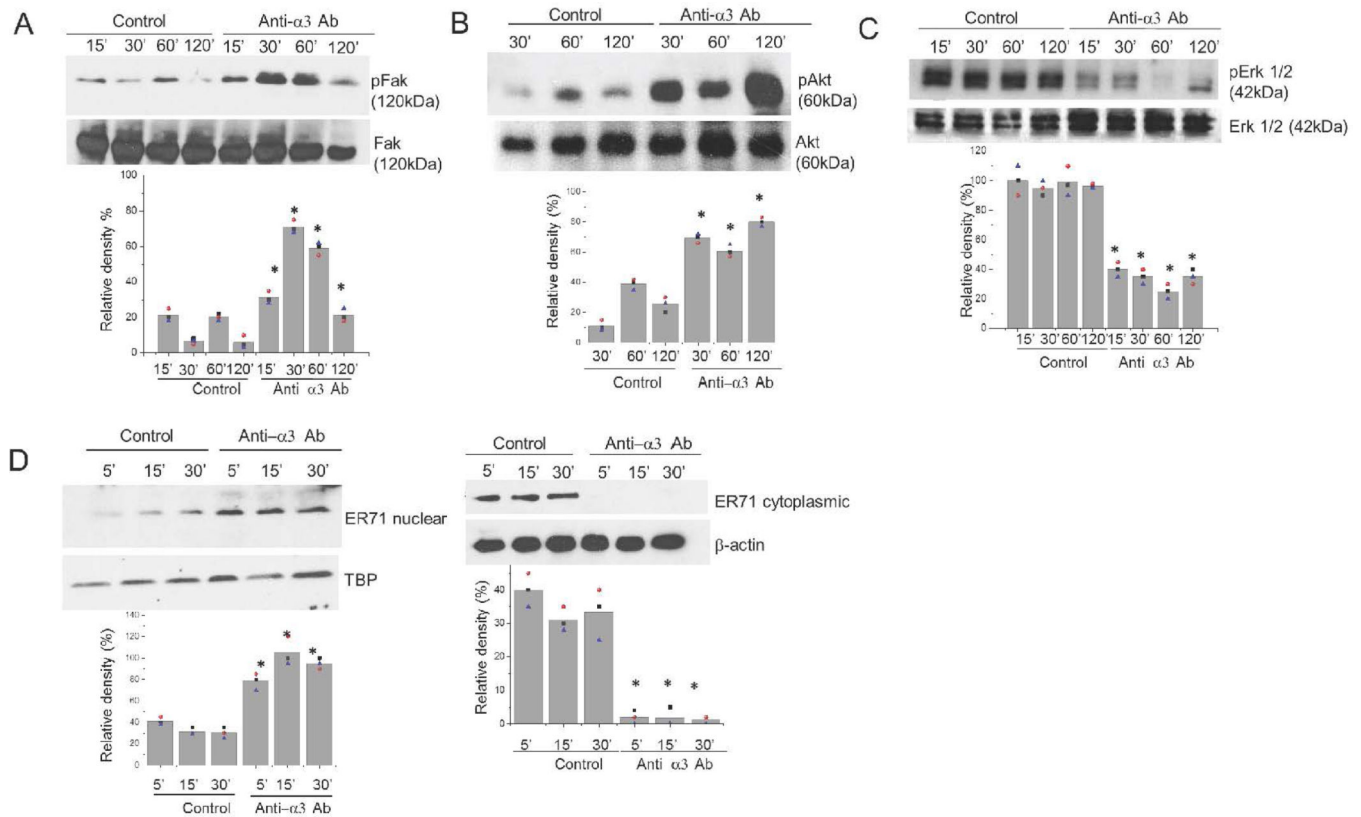


Figure 4. α 3 counteracts α 6 signaling to suppress EC lineage specification

(A–C) α 3 negatively regulates α 6 signaling in mESC differentiated on LN-1 as demonstrated by increased phosphorylation of FAK (p-Y576-FAK) (A) and Akt (B) and decreased activation of Erk1/2 (C) after exposure of day#3 mESCs (FACS-sorted for Flk1+) to 50 μ g/ml Ralpb 3.1 for various time points up to 120min. Error bars, mean \pm S.E.M.; * $P < 0.05$ for comparisons between α 3 blocked cells vs. controls, $n = 3$.

(D) Left. α 3 negatively regulates Er71 translocation to nuclei of mESC differentiating to ECs. Day#3 differentiating mESCs (FACS-sorted for Flk1+) exposed to 50 μ g/ml Ralpb 3.1 for the indicated times or controls were collected and lysed, and cytoplasmic and nuclear extracts prepared. Nuclear extracts were immunoblotted with anti-Er71 and anti-TATA-Binding Protein (TBP) antibodies. Bar graph represents densitometric quantitation from 3 individual experiments; error bars, mean \pm S.E.M.; * $P < 0.05$ for α 3 blocked cells vs. controls. Right. α 3 promotes retention of Er71 in the cytosol. Cytoplasmic fractions were immunoblotted with anti-Er71 and anti- β -actin. Bar graph represents densitometric quantitation. Error bars, mean \pm S.E.M.; * $P < 0.05$ for α 3 blocked cells vs. controls, $n = 3$.

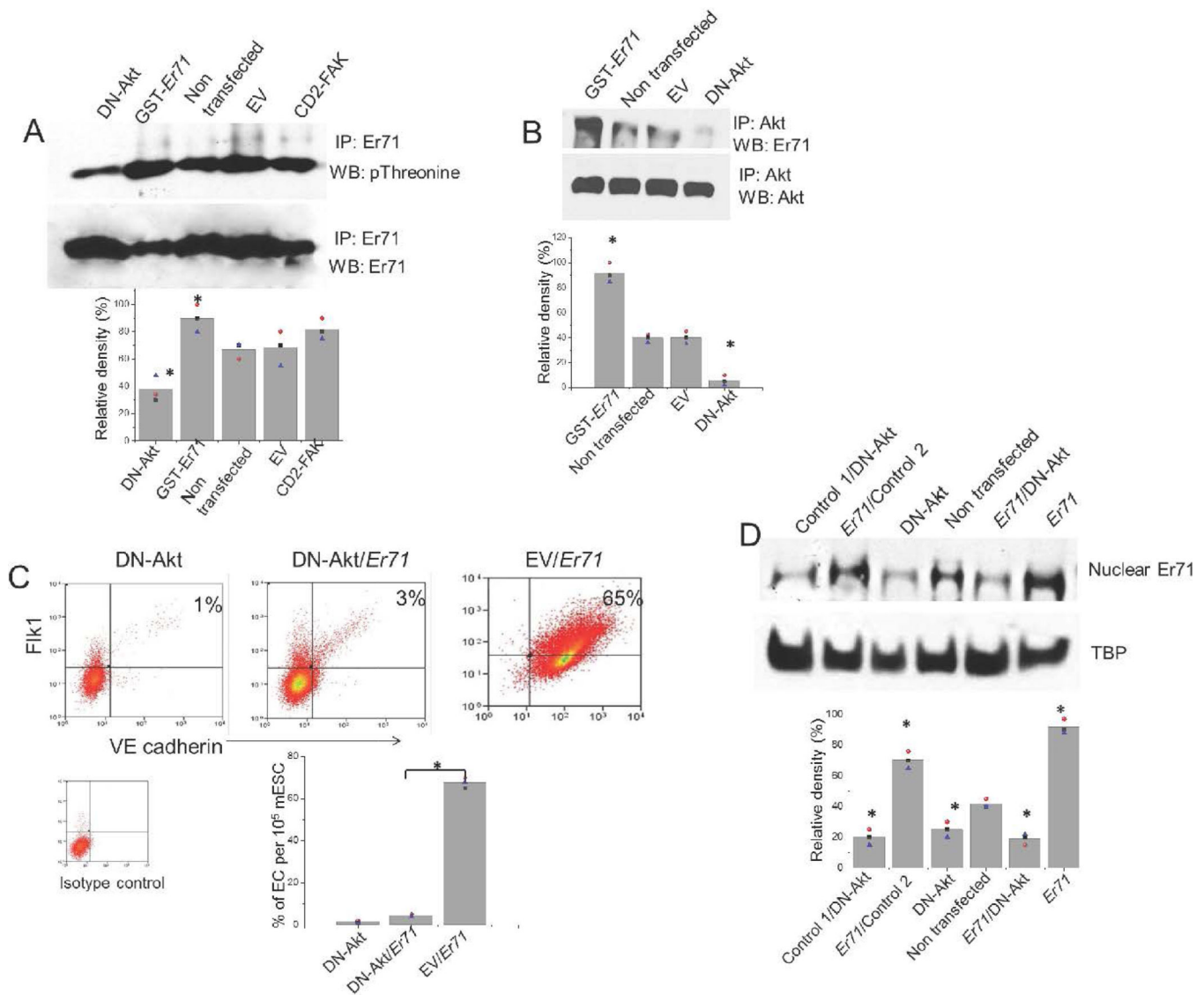


Figure 5. Akt mediates Er71 phosphorylation and induction of EC lineage transition

(A) Akt regulates Er71 phosphorylation. mESCs transfected with DN-Akt or empty vector (EV) were exposed to mesodermal differentiation conditions. As positive controls we used mESCs transfected with constitutively-active CD2-FAK or mESCs transfected with GST-*Er71* construct. At 15 min after exposure to VEGF165 containing media, the cells were lysed, immunoprecipitated with anti-Er71, and analyzed by indicated antibody. Error bars, mean \pm S.E.M., * $P < 0.05$ for comparisons between experimental groups vs. controls, $n = 3$.

(B) Activated Akt associates with Er71. mESCs transfected with DN-Akt, empty vector (EV) or GST-*Er71* were exposed to VEGF165 containing differentiation media for 30min, cells were lysed, immunoprecipitated with anti-Akt antibody and analyzed by WB with anti-Er71 antibody. Error bars, mean \pm S.E.M., * $P < 0.05$ for comparisons between experimental groups vs. controls, $n = 3$.

(C) mESCs were transfected with DN-Akt alone or combined with GST-*Er71* or DN-Akt empty vector (EV) combined with GST-*Er71* and were exposed to differentiation conditions

as per our standard protocol. After 6 days, cell surface expression of Flk1 and VE-cadherin (double positive) was examined by flow cytometry. Bar graph shows quantitation of Flk1⁺/VE-cadherin⁺ ECs under the 3 experimental conditions. Error bars, mean \pm S.E.M., * P<0.05 vs indicated conditions, n=3.

(D) Akt is required for Er71 localization to nuclear compartment during mESCs differentiation into ECs. mESCs were transfected with DN-Akt, GST-*Er71* or both, and were exposed to differentiation conditions as above. Controls were transfected with GST-empty vector (indicated as Control 1) and DN-Akt-empty vector (indicated as Control 2). At 1hr after exposure to VEGF165 in the differentiation media, cells were solubilized and the nuclear fraction used for WB against Er71. Error bars, mean \pm S.E.M., * P<0.05 for comparisons between experimental groups vs. controls, n=3.

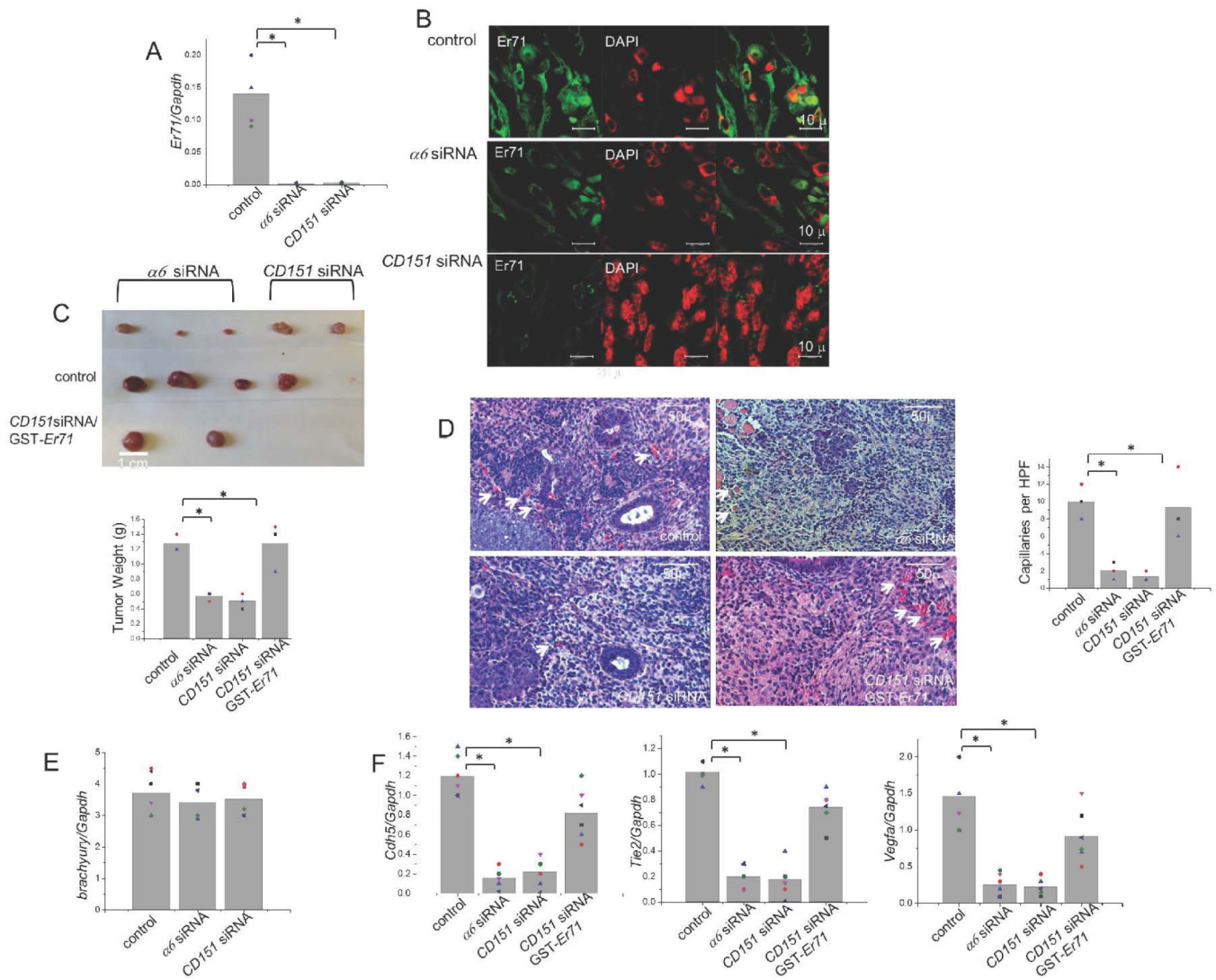


Figure 6. $\alpha 6$ /CD151 signaling induces Er71 activation and vasculogenesis in mice
 (A) mESCs transfected with indicated siRNAs as described in the Methods were transplanted subcutaneously in immunocompromised mice. The cell aggregates were removed 3 days later and quantification of *Er71*- and control *GAPDH*-transcripts levels was performed. Error bars, mean \pm S.E.M., * $P < 0.05$ vs. indicated conditions, $n = 6$.
 (B) Immunofluorescence staining of Er71 (green) performed on cryo-sections of day-3 cell aggregates isolated from mice as described in A. Staining of control sections showed presence of Er71 both in cytoplasmic and nuclear compartments, as demonstrated by co-localization with nuclear DAPI (red) staining. In $\alpha 6$ - or *CD151*-knockdown cells, however, the Er71 staining was reduced in the cytoplasm, and Er71 failed to localize in the nucleus. Scale bar, 10μ . Fluorescent images were acquired with a Zeiss LSM 710 META confocal laser scanning microscope using a C-Apochromat 63x/1.2NA objective, (2.6x Zoom factor).
 (C) Morphology and size of tumors removed 10 days after transplantation deriving from either control mESCs or mESCs transfected with either $\alpha 6$ - or *CD151*-siRNA or doubly

transfected with *CD151*-siRNA/*GST-ER71*. Bar graph depicts tumor weights (in g), bars represent mean \pm S.E.M., * $P < 0.05$, compared conditions are indicated by parentheses, $n=3$. (D) Teratomas were stained with H/E, and the vascular structures (pointed by arrow heads) were measured in each 20X field using a phase contrast microscope. The bar graph represents quantification of the tumor vascularity in the control mESC-derived tumors compared to *α6*- and *CD151*-knockdown mESC-derived tumors as well as in tumors derived from doubly transfected *CD151*-siRNA/*GST-ER71* mESCs, bars represent mean \pm S.E.M., * $P < 0.05$, compared conditions are indicated by parentheses, $n=3$.

(E) Quantification of *Brachyury*- and control *GAPDH*-transcripts levels in teratomas deriving from mESCs transfected with indicated siRNAs as described in the Methods ten days after subcutaneous transplantation in immunocompromised mice. Each tumor was divided in 6 parts and random parts were chosen for whole tissue RT-PCR. Error bars, mean \pm S.E.M., * $P < 0.05$ vs. indicated conditions, $n=6$.

(F) Quantification of *Cdh5Tie2*, *Vegfa*, and control *GAPDH*-transcript levels in teratomas derived from mESCs transfected with indicated siRNAs as described in Methods 10 days after subcutaneous transplantation in immunocompromised mice. Each tumor was divided in 6 parts and random parts were chosen for whole tissue RT-PCR. Error bars, mean \pm S.E.M., * $P < 0.05$ vs. indicated conditions, $n=6$.